Journal of Computer Science

Original Research Paper

Automatic Detection of the End-Diastolic and End-Systolic from 4D Echocardiographic Images

[1]Anas A. Abboud, [1]Rahmita Wirza Rahmat, [2]Suhaini Bin Kadiman, [3]Mohd Zamrin Bin Dimon, [1]Lili Nurliyana, [4]M. Iqbal Saripan and [1]Hasan H. Khaleel

[1]*Department of Computer Science and Information Technology, UPM, 43400, Serdang, Malaysia*
[2]*National Heart Institute (IJN), No 145 Jalan Tun Razak, 50400 Kuala Lumpur, Malaysia*
[3]*Faculty of Medicine, Universiti Teknologi MARA(UiTM), 47000, Sungai Buloh,Malaysia*
[4]*Department of Computer and Communication Systems Engineering, Faculty of Engineering, UPM, 43400, Serdang, Malaysia*

Article history
Received: 05-03-2014
Revised: 26-05-2014
Accepted: 09-08-2014

Corresponding Author:
Anas A. Abboud
Department of Computer Science and Information Technology,
University Putra Malaysia, 43400,
Serdang, Malaysia
Email: anasalabousyupm@gmail.com

Abstract: Accurate detection of the End-Diastolic (ED) and End-Systolic (ES) frames of a cardiac cycle are significant factors that may affect the accuracy of abnormality assessment of a ventricle. This process is a routine step of the ventricle assessment procedure as most of the time in clinical reports many parameters are measured in these two frames to help in diagnosing and dissection making. According to the previous works the process of detecting the ED and ES remains a challenge in that the ED and ES frames for the cavity are usually determined manually by review of individual image phases of the cavity and/or tracking the tricuspid valve. The proposed algorithm aims to automatically determine the ED and ES frames from the four Dimensional Echocardiographic images (4DE) of the Right Ventricle (RV) from one cardiac cycle. By computing the area of three slices along one cardiac cycle and selecting the maximum area as the ED frame and the minimum area as the ES frame. This method gives an accurate determination for the ED and ES frames, hence avoid the need for time consuming, expert contributions during the process of computing the cavity stroke volume.

Keywords: End-Diastolic (ED) and End-Systolic (ES), Echocardiography Image, Stroke Volume, Right Ventricle (RV), Left Ventricle (LV), Three Dimensional Echocardiography (3DE), Proposed Method, QLAB System, Automatic Algorithm, Wall Motion

Introduction

Accurate detection of the End-Distally (ED) and End-Systolic (ES) stages of a cardiac cycle is a significant factor that can affect the accuracy of abnormality assessment of a ventricle (Ostenfeld *et al*., 2012; Darvishi *et al*., 2012). This process is a routine step of the ventricle assessment procedures, where often, in clinical reports, many parameters can be measured in these two stages to help in diagnosing and decision making (Umberto *et al*., 2008). However, the process of detecting the ED and ES still a challenge for diagnosis because it was mostly done manually by tracking the cine loop during the clinical procedure, as in (Niemann *et al*., 2007) or by optical tracking of the change of ventricle dimensions through watching the individual image faces of the ventricle during the cardiac cycle, as in (Aune *et al*., 2009; Crean *et al*., 2011; Dawood *et al*., 2011).

Tracking the mitral valve motion is another method for detecting the ED and ES frame (Hussein *et al*., 2011), where the ES stage is defined as the last frame before the opening of the mitral valve while the ED stage is the last frame before the closing for the mitral valve, as reported by (Nosir *et al*., 1996). In the meanwhile, tracking the mitral valve together with the ventricle volume was presented by (Umberto *et al*., 2008). ECG signal was used by (Zhu *et al*., 2009) to determine the ED and ES frame of the LV in order to generate a dynamic model of the LV. (Gopal *et al*., 2007; Chua *et al*., 2009) also used ECG to determine the ED frame through the R wave of the ECG and the ES frame was determined as the smallest cavity area. The biggest and smallest area of the RV cavity were visually tracked in three views; short axis, four chamber and coronal by (Ostenfeld *et al*., 2012) to determine the ED and ES cardiac stages.

Gifani *et al*. (2010) presented an automatic detection method for ED and ES of LV from two and four chamber views using unsupervised learning algorithm (Locally Linear Embedding (LLE)) for three cardiac consecutive cycles. (Shalbaf *et al*., 2011) performed image registration for echocardiographic images of 6 volunteers, distance computation and finally the classical Multi-Dimensional Scaling (MDS) used to construct low dimensional representation of 2D LV images to generate Iso-map. Then, they computed manifold model of seven phases of cardiac cycles to determine ED and ES stages automatically.

(Yuanfang *et al*., 2011) determined ED and ES stages by tracking the mitral valve motion, based on (Nosir *et al*., 1996)'s definition for the ED and ES stages. This method used 3D echo image of LV, by binaries and enhancing images in the pre-processing stage of their algorithm. Then, a dilation operation for different resolution scale was performed to avoid the blood flow effect. Finally, the number of connecting regions for 8-neighbore connectivity was computed. This method gives accurate results only with good quality echo image of mitral valve.

All of methods reviewed in this literature are time consuming; therefore, an accurate automatic detection for the ED and ES stages is highly required to assist specialists and interns in their clinical work.

Materials and Methods

The main goal of the proposed method is to enable automatic detection of the ED and ES frames from one cardiac cycle. This process is one of the steps of the main algorithm for measuring the RV stroke, which proposed automatic measuring for the ventricle stroke volume. Whereby the ventricle stroke volume is the volume of blood ejected from a ventricle at each beat of the heart. This is equal to the difference between the cavity volume at the End-Diastolic stage (EDV) and the cavity volume of at the End-Systolic stage (ESV) of the cardiac cycle according to (Barash *et al*., 2011). This requires the determination of the ED and ES frames of the cardiac cycle and measuring the cavity volume at the end-diastolic and end-systolic as stated by (Klabunde, 2011).

The cardiac cycle duration (or the number of frames in a cardiac cycle) is different from one patient to another. The ES frame position in the echocardiography video of a cardiac cycle (the ES stage of a cardiac cycle) is also different from one patient to another, as illustrated in Table 1. The ED frame as determined by the experts can be used as the first image in the cardiac cycle. It can also be considered as the frame following closure of the mitral valve, or the frame of the largest cavity in the cardiac cycle.

An automatic detection of the ED-ES frames is proposed, by measuring the area of the segmented cavity of the RV along a cardiac cycle for three slices in the middle region of the RV, as in Equation 1:

$$Area_{s(r)} = \sum_{i=1}^{n} \sum_{j=1}^{m} f(i,j),\ for\ all\ f(i,j) > 0 \qquad (1)$$

where, $Area_{s(r)}$ is the area of the segmented region in slice number r, where r = 8, 9, 10 and $f(i,j)$ is the grayscale of the pixels in the segmented region.

These three slices (8, 9 and 10) which are located in the middle region of the RV cavity as presented in Fig. 1, is selected based on analyzing the structure and motion behavior of the 16 slices over a cardiac cycle for the patients in the dataset, of the RV cavity.

The details of selecting these slices are explained in the following sub-section.

Slice Selection

Selecting the slices from the middle region of the RV cavity is based on two anatomical facts.

First; the free wall area of the RV cavity in the middle region (fractional region) is broader than the inflow and out flow tract as illustrated in Fig. 2 and 3.

Therefore, for fully automatic detection of the ED-ES frame, the middle region of the cavity is sliced for this purpose. The middle region has a close intracardiac boundary along the cardiac cycle, while the inflow and outflow tract is affected by the motion of the valves (opening and closing) during the cardiac cycle. When the valve is closed, the region will be closed and segmentation includes only the intra cavity region.

However, when the valve is open, the segmentation will be growing out of the inflow and/or outflow tract. Figure 3 illustrates the intracardiac boundary of the RV in inflow, middle and out flow regions along different frames of one cardiac cycle video, for a patient.

Second; the amount of changes in the cavity area, in the middle region during the cardiac cycle is higher than the changes of the inflow and outflow tract. To experiment with this fact, the area of the 16 slices is computed for one cardiac cycle for one sample patient of the dataset.

Then the standard deviation and variance of the changing for total area of the cavity in each slice are computed for the comparison of each slice in one cardiac cycle. This is illustrated in Table 1-4 respectively and the corresponding diagram in Fig. 4-6, respectively for a sample of three patients of the data set.

The Tables and Diagrams clearly show that the middle region is highly affected along the cardiac cycle for which to be a candidate it has to be a good indicator of the ED and ES cardiac cycle frames.

By averaging the three previous samples, it can be concluded that the middle region has the highest fractional region (the region with maximum change in the cavity during the cardiac cycle), this is illustrated in Fig. 7.

Selecting the ED-ES Frames

In the proposed method, three slices are used to detect the ED and ES frames, as using three frames may provide accurate detection of the ED and ES frames. The diagram in Fig. 8 illustrates the method of detecting the ED and ES frames of the cardiac cycle.

As stated earlier in the proposed method, three slices are used to determine the frames of the ED and the ES stages. The reason for selecting three slices can be justified by computation analysis as in the following steps.

Compute the change in the area of the segmented region in the frame ρ and compare it with the area of the frame ρ-1 of the same slice, for each of the three slices, as shown in Table 4.

According to the definition of the ED Frame, the maximum area of the segmented region is tracked from Table 4. The segmented areas for each of three slices (8, 9 and 10) in the first row are compared with its area in the second row. We can see that; for the slice number 8 the area is decrease in the second row and for slice number 9 and 10 the area increase in the second row, however the average of the area of the tree slices still the highest in the first row, thus we use the frame number in the first row as the ED stage of the cardiac cycle. Therefore the frame of first row can be considered as the ED frame.

By tracing the changes of the area, the minimum area in each slice falls in different frame numbers. For example in the segmented region area of slice 10, the area decreases in the frame 10, 11, until it reaches the minimum area in frame 12 and it starts to increase again in frame 13, as illustrated in Fig. 9. However, the segmented region area of slice 9 increases in frame 10, decreases to the minimum in frame 11 and then continues increasing in frames 12, 13… and so on. This procedure shown in Table 4 by the arrows.

To satisfy the accuracy of determining the ED and ES frames, the mean of the area is computed for three slices using Equation 2 and Equation 3 and the result is shown in Fig. 10.

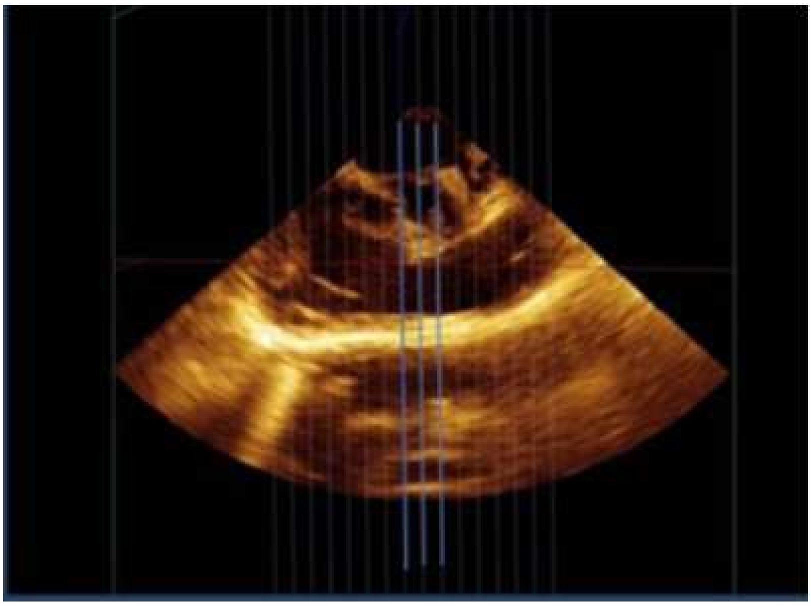

Fig. 1. Three slices from the middle region of the RV cavity. Slice 8, Slice 9 and Slice 10 from left to right

DOI: 10.3844/jcssp.2015.230.240

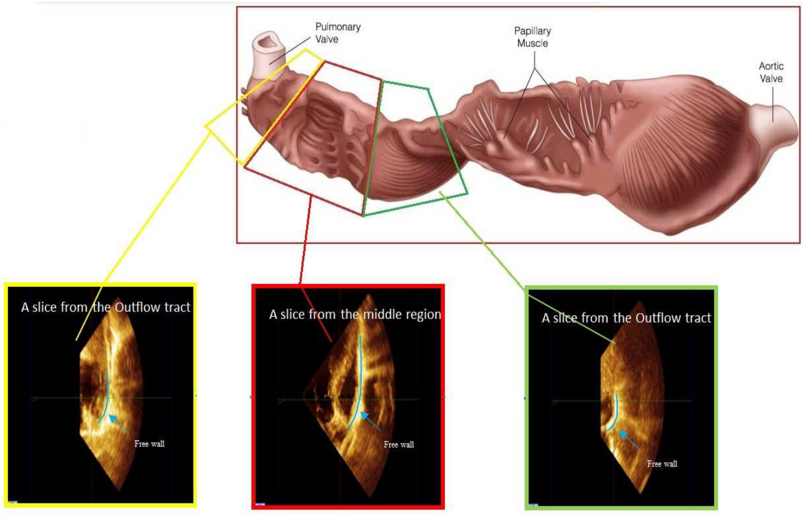

Fig. 2. Right ventricle slices at inflow, middle and outflow regions of RV cavity

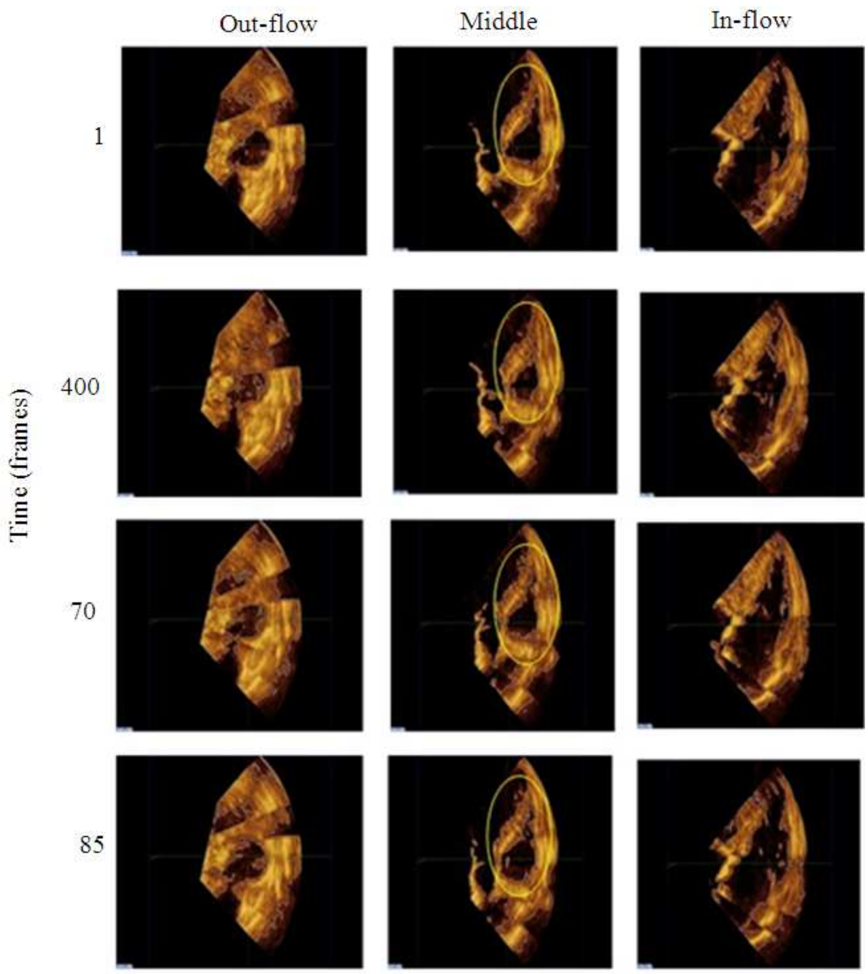

Fig. 3. The three regions (Inflow-Middle-Outflow) of the RV cavity for one patient of the data set, explain the changes in the cavity during a cardiac cycle and the effect of opening the TV and PV. The RV cavity boundary in the middle region (highlighted) is closed in the middle during the cardiac cycle

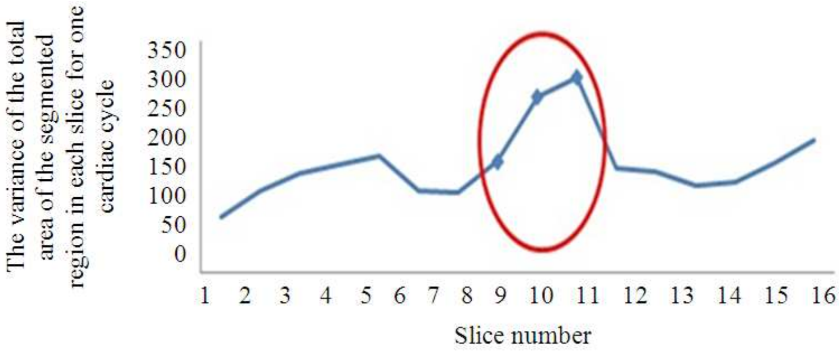

Fig. 4. Diagram of changing in the cavity area in each slice during one cardiac cycle for Patient 1

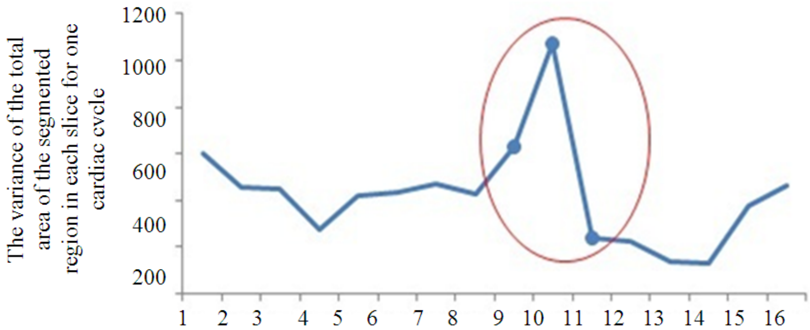

Fig. 5. Diagram of changing in the cavity area in each slice during one cardiac cycle for Patient 2

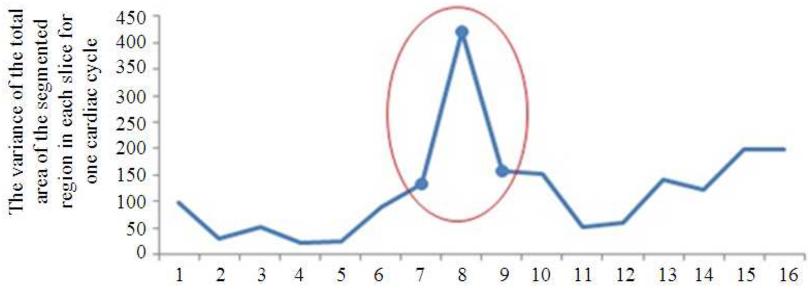

Fig. 6. Diagram of changing in the cavity area in each slice during one cardiac cycle for Patient 3

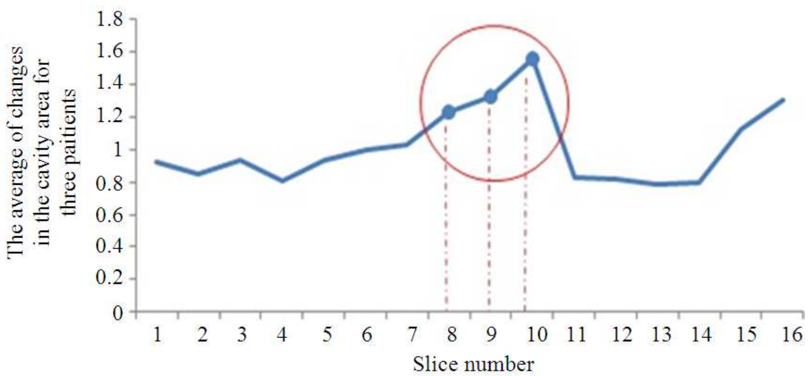

Fig. 7. Average of the standard deviation of the three patients, illustrating that the middle region is the greatest changing region affected in the cavity during the cardiac cycle

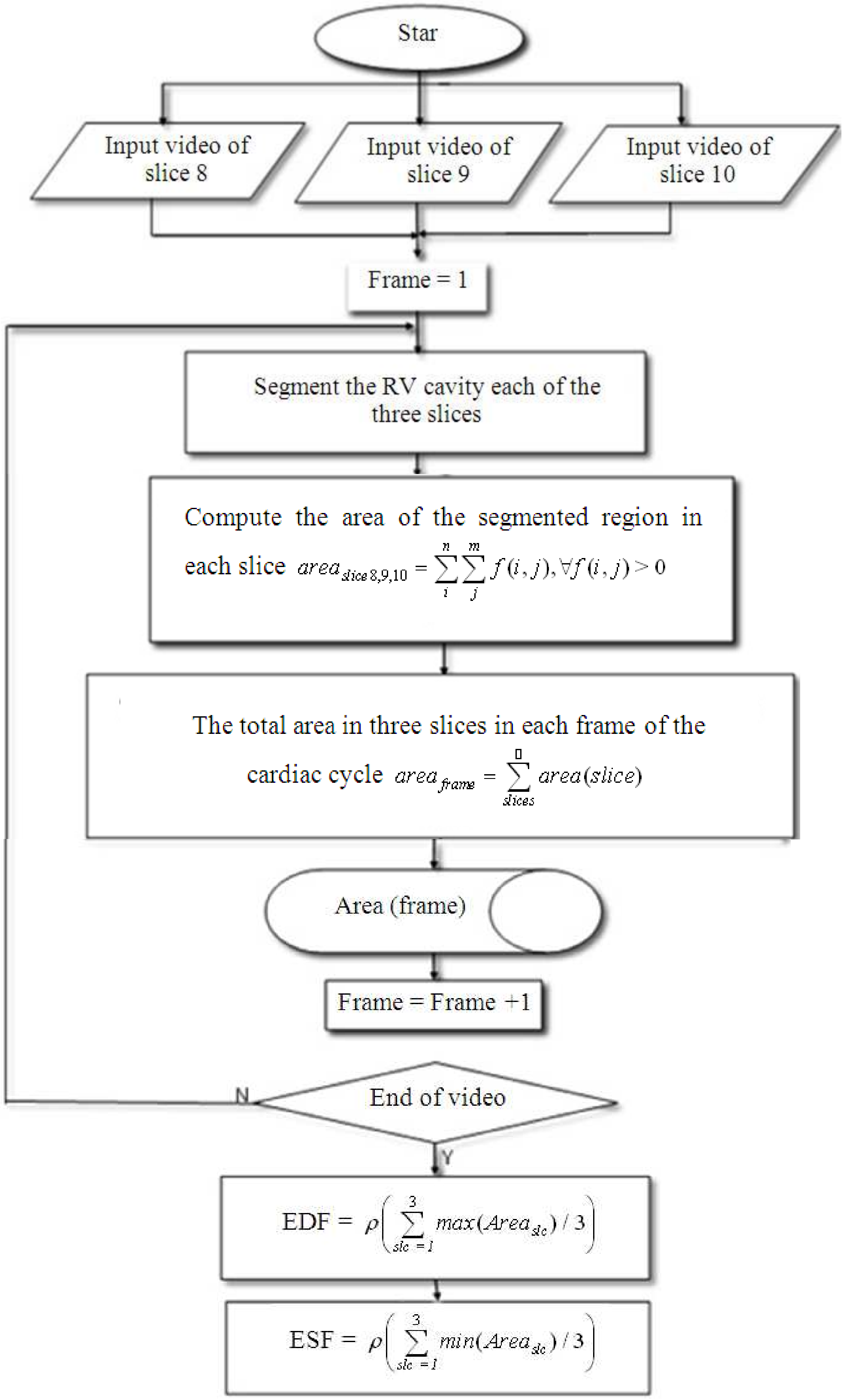

Fig. 8. Diagram of the method of the determination of ED and ES

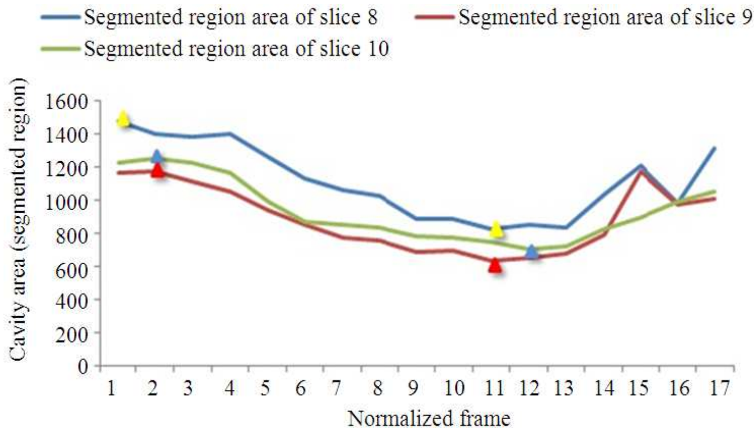

Fig. 9. The area of three slices (8, 9 and 10) during the cardiac cycle

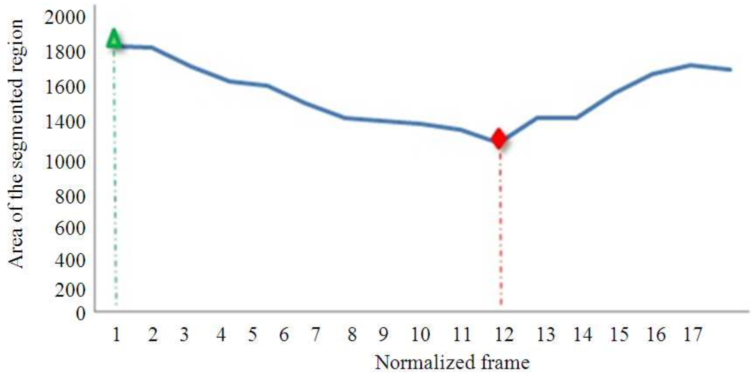

Fig. 10. The mean of areas for the three slices (8, 9 and 10) and the frames, the maximum area indicates the ED frame and the minimum area indicates the ES frame

Table 1. The changes of the cavity area for Patient 1, during one cardiac cycle in each slice (Si) are the slices I =1 to 16, Ni is the frames of one cardiac cycle video

N.Frame	S1	S2	S3	S4	S5	S6	S7	S8	S9	S10	S11	S12	S13	S14	S15	S16
N1	820	927	982	950	1195	909	817	960	1120	1247	1041	1233	1287	1435	928	1263
N2	700	802	881	998	1200	996	884	852	1092	1364	1091	1239	1311	1347	1002	1277
N3	726	745	832	972	1093	990	843	754	902	1064	1092	1111	1182	1264	916	900
N4	766	766	766	851	1013	915	804	658	679	973	854	1078	1140	1188	846	830
N5	796	664	660	726	906	850	718	592	584	916	756	953	1094	1054	603	735
N6	774	620	579	652	820	830	670	529	479	839	664	1017	1090	981	597	696
N7	685	573	530	630	790	801	638	542	416	485	688	973	926	1022	552	658
N8	654	548	536	657	772	783	586	490	510	504	726	1176	1302	1289	553	706
N9	599	554	543	687	787	807	599	492	402	508	788	1211	1348	1300	501	678
N10	603	551	518	580	721	778	584	508	388	498	765	1164	1404	1347	592	738
N11	603	556	534	520	779	608	577	413	344	446	632	843	1358	1290	597	742
N12	634	585	614	504	738	566	565	392	354	855	695	805	1125	1338	620	800
N13	684	667	620	596	637	706	484	419	579	855	679	822	1266	1151	609	742
N14	858	847	785	792	881	763	646	607	824	940	825	996	1170	1131	778	907
Variance	7255	15713	23065	27338	31697	15764	14836	28407	70943	87740	24971	23251	17619	19059	27425	39833
STDV	85	125	152	165	178	126	122	169	266	296	158	152	133	138	166	200

$$EDF = \rho \frac{\sum_{slc=1}^{3} Max(area_{slc})}{3} \quad (2)$$

$$ESF = \rho \frac{\sum_{slc=1}^{3} min(area_{slc})}{3} \quad (3)$$

where, is an indicator of the position of the frames in the cardiac cycle video, as declared in Table 6, EDF is the end diastolic frame, ESF is the end systolic frame and $Area_{slc}$ is the area of the segmented region of the cavity in the slice.

For the sample data used in Fig. 9 and 10, the number of frames in one cardiac cycle is 68 frames. According to the computed segmented area and the frames, ES frame ρ = 11 is frame number 41 in the video.

Table 2. The changes of slice area for Patient 2, during one cardiac cycle (Si) are the slices I =1 to 16, Ni is the frames of one cardiac cycle video

	S1	S2	S3	S4	S5	S6	S7	S8	S9	S10	S11	S12	S13	S14	S15	S16
N1	1763	1728	1678	1559	1776	1733	1854	1864	1854	2241	2620	2899	2615	2265	1950	1600
N2	1794	1739	1713	1573	1805	1689	1830	1458	1499	2208	2568	2871	2621	2273	2015	1695
N3	1860	1751	1694	1562	1780	1668	1720	1406	1515	2141	2508	2800	2461	2026	1724	1478
N4	1721	1649	1554	1509	1679	1582	1635	1329	1385	1988	2426	2716	2445	2052	1750	1573
N5	1540	1495	1346	1360	1454	1475	1608	1611	1248	1475	2261	2690	2453	2044	1813	1648
N6	1440	1363	1278	1318	1386	1338	1445	1511	1162	1293	2183	2578	2393	1971	1643	1562
N7	1353	1267	1231	1264	1328	1271	1335	1394	1089	1318	2225	2459	2334	1966	1589	1411
N8	1278	1230	1177	1206	1280	1228	1328	1373	1056	1251	2182	2494	2293	1884	1540	1396
N9	1216	1173	1167	1175	1262	1210	1279	1365	1056	1429	2246	2459	2262	1968	1470	1374
N10	1175	1170	1145	1110	1262	1223	1276	1312	1023	1463	2169	2469	2273	1952	1501	1144
N11	1168	1214	1180	1160	1305	1280	1247	936	1052	1777	2137	2429	2271	1943	1463	1068
N12	1105	1178	1191	1146	1314	1323	1209	1305	1269	1730	2175	2479	2335	1952	1468	980
N13	1222	1202	1190	1199	1342	1114	1253	1291	1250	1631	2253	2569	2256	1888	1318	1061
N14	1390	1328	1328	1256	1459	1235	1461	1406	1452	1706	2277	2579	2348	1881	1436	1330
N15	1564	1439	1484	1417	1600	1567	1578	1575	1612	1813	2342	2674	2379	1990	1528	1279
N16	1604	1500	1558	1482	1660	1626	1621	1616	1719	1946	2427	2649	2442	2041	1681	1364
N17	1638	1536	1610	1515	1719	1685	1730	1719	1325	2053	2511	2764	2518	2067	1819	1498
Var.	59980	45367	44613	27405	41775	43767	47212	42437	63179	107029	24103	22794	13406	12864	37336	46398
STDV	244	213	211	165	204	209	217	206	251	327	155	150	115	113	193	215

Table 3. The changes of slice area for Patient 3, during one cardiac cycle (Si) are the slices I =1 to 16, Ni is the frames of one cardiac cycle video

	S1	S2	S3	S4	S5	S6	S7	S8	S9	S10	S11	S12	S13	S14	S15	S16
N1	2027	1488	968	1127	932	1105	1317	1502	1812	1874	1928	1894	2101	2061	1947	1219.00
N2	1944	1482	971	1124	941	1106	1298	1530	1579	1678	1942	1922	2322	2052	1915	1160.00
N3	1693	1493	949	1132	970	1121	1337	1526	1552	1781	1951	1924	2322	2023	1883	1122.00
N4	1757	1441	920	1119	978	1115	1222	1443	1516	1512	1881	1873	2257	2009	1853	1093.00
N5	1828	1390	945	1117	1050	1068	1202	1344	1466	1393	1779	1778	1879	1880	1828	1063.00
N6	1859	1397	945	1101	1007	953	1188	1310	1435	1339	1748	1640	2005	1803	1814	1022.00
N7	1847	1429	921	1098	969	909	1156	1263	1532	1302	1949	1772	2148	1888	1815	992.00
N8	1805	1479	909	1085	961	859	1092	1197	1347	1396	1955	1812	1984	1919	1825	953.00
N9	1749	1425	907	1078	950	848	1096	1145	1596	1571	2000	1888	2008	1984	1820	917.00
N10	1662	1408	907	1046	947	844	1072	1059	1622	1503	1977	1916	2039	1989	1750	874.00
N11	1691	1415	866	1059	965	888	1057	1021	1437	1646	1951	1883	2060	2012	1726	864.00
N12	1675	1387	833	1122	970	938	1019	966	1459	1541	2108	1858	2044	2022	1692	822.00
N13	1657	1385	817	1138	974	843	1003	952	1621	1551	2113	1861	2062	1990	1666	793.00
N14	1629	1373	814	1060	1024	850	940	972	1651	1567	1994	1893	2035	1949	1629	778.00
N15	1644	1314	819	1126	1015	870	941	1115	1684	1691	2001	1934	2084	1911	1605	807.00
N16	1642	1305	825	1129	1073	966	1062	1143	1713	1696	2016	1978	2060	1908	1575	792.00
N17	1617	1331	822	1204	1061	998	1108	1132	1795	1670	1955	1959	2021	1728	1547	750.00
N18	1645	1378	841	1159	1090	1030	1127	1157	1837	1637	1922	1783	1853	1707	1494	710.00
N19	1645	1338	880	1203	1092	1020	1158	1205	1808	1441	1993	1756	1816	1719	1490	755.00
N20	1632	1421	960	1168	1072	948	1082	1245	1547	1472	1988	1756	1876	1737	1496	804.00
N21	1611	1456	1008	1191	1037	948	1093	1313	1712	1487	2011	1765	1918	1781	1503	832.00
N22	1700	1472	1024	1192	1037	1058	1264	1393	1761	1504	1995	1757	1915	1738	1507	863.00
N23	1700	1409	1004	1213	1059	1046	1245	1428	1721	1558	1920	1769	1923	1743	1535	923.00
N24	1678	1423	1022	1207	1007	1089	1270	1453	1790	1584	1932	1792	1917	1788	1571	1030.00
N25	1669	1456	1012	1191	1046	1071	1281	1493	1700	1587	1920	1733	1934	1788	1587	1032.00
N26	1661	1421	1009	1198	978	1074	1271	1477	1670	1586	1929	1814	1933	1798	1631	1062.00
N27	1677	1428	1000	1175	973	1058	1257	1480	1697	1610	1961	1828	1955	1814	1682	1065.00
N28	1645	1421	983	1174	1001	1085	1254	1492	1643	1590	1966	1863	2014	1854	1712	1082.00
N29	1642	1418	981	1157	947	1053	1255	1500	1663	1568	1942	1829	2019	1879	1744	1076.00
N30	1666	1440	974	1158	939	1079	1273	1498	1680	1570	1940	1777	1986	1900	1786	1070.00
N31	1629	1451	987	1162	934	1089	1293	1632	1672	1582	1916	1765	1971	1887	1830	1075.00
N32	1613	1534	1009	1152	939	1084	1307	1609	1646	1623	1911	1869	2032	1918	1847	1077.00
N33	1715	1540	1029	1154	962	1109	1313	1596	1826	1795	2043	1911	2059	2036	1864	1087.00
Var.	9707	3088	5129	2121	2486	9088	13227	41985	15755	15279	5071	5854	14033	12125	19847	19723.00
STDV	98	55	71	46	49	95	115	204	125	123	71	76	118	110	140	140.44

Results

The proposed method was implemented on an LV dataset of 12 patients. The ED and ES of these data were determined by cardiologists from the National Heart Institute (IJN, KL. Malaysia), during a routineclinicalassessment. Using the current available software A-QLAB, the proposed method was implemented on the LV dataset, although the A-QLAB software was designed for quantifying the LV and mitral valve. The ED and ES Frames were determined manually by the expert during the routine clinical test for 12 patients. By default, the expert assumed the ED was the first frame of the cardiac cycle for all patients' data. The ES was determined by visual tracing of the cavity area changes and mitral valve together by considering the frame with the minimum area of the cavity and a closed mitral valve. The ED and ES frames that were selected by the experts and determined automatically by the proposed method were recorded and shown in Table 5.

Table 4. Computed area for three slices and the average, the rows indicate the changes in the area of the segmented region of the frame ρ compared with frame ρ-1

Normalized frame (Indicator) ρ	The frame position in the cardiac cycle	Segmented region area of slice 8	Segmented region area of slice 9	Segmented region area of slice 10	Mean of area
1	1	1476	1160	1226	1732
2	5	1401↓	1173↑	1248↑	1730
3	9	1378	1111	1225	1604
4	13	1396	1053	1163	1508
5	17	1258	933	989	1480
6	21	1125	846	865	1363
7	25	1062	771	851	1262
8	29	1020	754	834	1246
9	33	886	685	783	1229
10	37	889↑	693↑	769	1188
11	41	826↓	633↓	743↓	1098
12	43	854↑	649↑	702↓	1262
13	47	836↓	677↑	722↑	1265
14	51	1036↑	785↑	825↑	1429
15	55	1210	1171	896	1549
16	59	982	971	990	1607
17	63	1314	1005	1051	1582

Table 5. Determining the position of the ED and ES frame in the video of a cardiac cycle for 12 patients

	Manual (by expert)		Automatic (proposed method)	
Patient no.	ED	ES	ED	ES
1	1	24	1	24
2	1	34	2	34
3	1	41	1	41
4	1	31	5	31
5	1	39	1	39
6	1	25	1	25
7	1	43	5	43
8	1	37	1	37
9	1	32	1	32
10	1	58	1	58
11	1	32	1	32
12	1	35	1	35

Table 6. Computing the EDA, to assess the effect of the variance in the frame number between the manual and the proposed automatic method. *e* is the absolute difference between the EDA of experts and automatic method

	Manual method			Automatic method			
Frame detection Method	Cardiac stage			Cardiac stage			Absolute difference between the EDA
Patient no.	ED frame no.	EDA	ES frame no.	ED frame no.	EDA	ES frame no.	of two methods (e)
P1	1	94	24	1	99	24	5
P2	1	141	34	2	134	34	7
P3	1	130	41	1	121	41	9
P4	1	104	31	5	110	31	6
P5	1	98	39	1	100	39	2
P6	1	93	25	1	97	25	4
P7	1	81	43	5	87	43	6
P8	1	137	37	1	132	37	5
P9	1	89	32	1	93	32	4
P10	1	99	58	1	98	92	1
P11	1	86	32	1	86	32	0
P12	1	90	35	1	90	35	0

From Table 5, it can be pointed out that the ES frames which were determined by the proposed method matches the ES frames which were selected by the experts for all of the 12 patients in the dataset.

Discussion

The result for ED frame selection is different between the proposed method and the experts by 2.5% of the data set (as in 2nd, 4th and 7th patients).

To analyse the effect of these difference in selecting the ED frames for these three patients P2, P5 and P7 using the proposed automatic method and the ED frame that selected manually by the experts for these three patients P2, P5 and P7. The absolute difference of the area of the cavity region in the End Dystonic frame (EDA) for both (automatic and manual) methods (e) is computed as declared in Table 6. Then the cavity volume at the ED is computed for the cases that have an error in detecting the ED frame for the patients P2, P5 and P7 is 0.05 mL, 0.077 mL and 0.04 mL respectively, regarding to the LV volume at End-Diastolic frame (EDV = 120 mL) according to (Schlosser *et al*., 2005) and (Blalock *et al*., 2013) this values represent 0.4, 0.6 and 0.3% of the EDV volume, which is a very small value and can be neglected.

Conclusion

This research is presented to explain the proposed algorithm of the automatic ED and ES frame detection from one cardiac cycle based on the medical definition of the ED as the maximum volume of the cavity and the ES as the minimum cavity volume in the cardiac cycle. By computing the segmented area for three slices in the middle region of the RV cavity, this region is selected after analysing the changes in the cavity area in three regions of the cavity Inflow, Middle and Outflow regions. The middle region was the most significant part in the changing area along a cardiac cycle and not the inflow and outflow tract. That is because the area of the free wall in this region is wider than the area of the free wall in the inflow and outflow tract, as illustrated in Fig. 2.

The cavity region is segmented for the three slices, along the video of one cardiac cycle and then the average of the slice area is computed. The frames of the maximum area and minimum area are detected as the ED and ES frames respectively. The results of the proposed algorithm have been validated using the A-QLAB system and datasets of different patients.

Funding Information

The authors have no support or funding to report.

Author's Contributions

All authors equally contributed in this work.

Ethics

This article is original and contains unpublished material. The corresponding author confirms that all of the other authors have read and approved the manuscript and no ethical issues involved.

References

Aune, E., M. Baekkevar, O. Rodevand and J.E. Otterstad, 2009. The limited usefulness of real-time 3-dimensional echocardiography in obtaining normal reference ranges for right ventricular volumes. Cardiovascular Ultrasound, 7: 35-35. DOI: 10.1186/1476-7120-7-35

Barash, P.G., B.F. Cullen, R.K. Stoelting, M.C. Stock and M.K. Cahalan, 2011. Clinical anesthesia. 1st Edn., Lippincott Williams and Wilkins, ISBN-10: 1451122977, pp: 1760.

Blalock, S., F. Chan, D. Rosenthal, M. Ogawa and D. Maxey *et al*., 2013. Magnetic resonance imaging of the right ventricle in pediatric pulmonary arterial hypertension. Pulmonary Circulat., 3: 350-355. DOI: 10.4103/2045-8932.114763

Chua, S., R.A. Levine, C. Yosefy, D.M. Handschumacher and J. Chu *et al*., 2009. Assessment of right ventricular function by real-time three-dimensional echocardiography improves accuracy and decreases interobserver variability compared with conventional two-dimensional views. Eur. J. Echocardiography, 10: 619-624. DOI: 10.1093/ejechocard/jep013

Crean, A.M., N. Maredia, G. Ballard, R. Menezes and G. Wharton *et al*., 2011. 3D Echo systematically underestimates right ventricular volumes compared to cardiovascular magnetic resonance in adult congenital heart disease patients with moderate or severe RV dilatation. J. Cardiovascular Magnetic Resonance, 13: 78-78. DOI: 10.1186/1532-429X-13-78

Dawood, T., M.P. Schlaich, N. Straznicky, M. Grima and C. Ika-Sari *et al*., 2011. Renal denervation: A potential new treatment modality for polycystic ovary syndrome. J. Hypertens., 29: 991-996. DOI: 10.1097/HJH.0b013e328344db3a

Darvishi, S., H. Behnam, M. Pouladian and N. Samiei, 2012. Measuring left ventricular volumes in two-dimensional echocardiography image sequence using level-set method for automatic detection of end-diastole and end-systole frames. Res. Cardiovasc Med., 1: 39-45. DOI: 10.5812/cardiovascmed.6397

Gifani, P., H. Behnam, A. Shalbaf and Z.A. Sani, 2010. Automatic detection of end-diastole and end-systole from echocardiography images using manifold learning. Phy. Measure., 31: 1091-1091. DOI: 10.1088/0967-3334/31/9/002

Gopal, A.S., O. Ebere, C.J. Chizor, I.S. Alan, K. S. Rena and T.W. Schapiro *et al*., 2007. Normal values of right ventricular size and function by real-time 3-dimensional echocardiography: Comparison with cardiac magnetic resonance imaging. J. Am. Soci. Echocardiography, 20: 445-455. DOI: 10.1016/j.echo.2006.10.027

Hussein, S.M., N.N. Batada, S. Vuoristo, R.W. Ching and R. Autio *et al*., 2011. Copy number variation and selection during reprogramming to pluripotency. Nature, 471: 58-62. DOI: 10.1038/nature09871

Klabunde, R. 2011. Cardiovascular physiology concepts. Cardiovascular physiology concepts. 1st Edn., Illustrated, Lippincott Williams and Wilkins, Philadelphia, ISBN-10: 1451113846, pp: 243.

Niemann, P.S., L. Pinho, T. Balbach, C. Galuschky, M. Blankenhagen and M. Silberbach *et al*., 2007. Anatomically oriented right ventricular volume measurements with dynamic three-dimensional echocardiography validated by 3-tesla magnetic resonance imaging. J. Am. Coll. Cardiol., 50: 1668-1676. DOI: 10.1016/j.jacc.2007.07.031

Nosir, Y.F.M., P.M. Fioretti, W.B. Vletter, B.E. Boersma and A. Salustri *et al*., 1996. Accurate measurement of left ventricular ejection fraction by three-dimensional echocardiography a comparison with radionuclide angiography. Circulation, 94: 460-466. DOI: 10.1161/01.CIR.94.3.460

Ostenfeld, E., M. Carlsson, K. Shahgaldi, A. Roijer and J. Holm, 2012. Manual correction of semi-automatic three-dimensional echocardiography is needed for right ventricular assessment in adults; validation with cardiac magnetic resonance. Cardiovascular Ultrasound, 10: 1-1. DOI: 10.1186/1476-7120-10-1

Schlosser, T., K. Pagonidis, C.U. Herborn, P. Hunold and K.U. Waltering *et al*., 2005. Assessment of left ventricular parameters using 16-MDCT and new software for endocardial and epicardial border delineation. Am. J. Roentgenol., 184: 765-773. DOI: 10.2214/ajr.184.3.01840765

Shalbaf, A., H. Behnam, P. Gifani and Z. Alizadeh-Sani, 2011. Automatic detection of end systole and end diastole within a sequence of 2-D echocardiographic images using modified Isomap algorithm. Proceedings of the 1st Middle East Conference on Biomedical Engineering, Feb. 21-24, IEEE Xplore Press, Sharjah, pp: 217-220. DOI: 10.1109/MECBME.2011.5752104

Umberto, B., M. Davide and S. Ovidio, 2008. Automatic computation of left ventricle ejection fraction from dynamic ultrasound images. Patt. Recognit. Image Anal., 18: 351-358. DOI: 10.1134/S1054661808020247

Yuanfang, G., V. Yao, K. Tsui, M. Gebbia and M.J. Dunham *et al*., 2011. Nucleosome-coupled expression differences in closely-related species. BMC Genom., 12: 466-466. DOI: 10.1186/1471-2164-12-466

Zhu, Y., X. Papademetris, J.S. Albert and S.D. James, 2009. A Dynamical Shape Prior for Lv Segmentation from RT3D Echocardiography. In: Medical Image Computing and Computer-Assisted Intervention-MICCAI, Yang, G.Z., D. Hawkes, D. Rueckert, A. Noble, C. Taylor (Eds.)., Springer Berlin Heidelberg, ISBN-10: 978-3-642-04267-6, pp: 206-213.